Surface Re-Esterification and Photo Sintering of Titania Xerogel Thin Films

Jeffrey R. S. Brownson, Tim J. Lee, and Marc A. Anderson*

Environmental Chemistry and Technology Program, University of Wisconsin— Madison, 660 North Park Street, Madison, Wisconsin 53706

Received January 13, 2005. Revised Manuscript Received April 11, 2005

Supraband gap light (<378 nm) was found to induce the hardening of films for surface-functionalized nanoparticles in titania xerogel thin films. Anatase nanoparticles prepared in acidic aqueous solutions and subsequently diluted in ethanol/water molar ratios >1 were re-esterified at the surface prior to UV exposure, as confirmed by Fourier Transform IR spectroscopy. Relative hardness tests demonstrated that sols having a high ethanol content, which are subsequently cast into thin films and subjected to UV light exposure under humid conditions, are capable of being hardened. The hardening effect was reduced relative to unexposed xerogel films at all tested humidity levels lacking UV exposure, indicating particle peptization without interparticle bonding. Contact angles significantly decreased for all films exposed to UV light. In contrast, films held in the dark did not change contact angles. Atomic force microscopy indicated nanoparticle growth for UV-exposed films at 40% relative humidity/40 °C. Adsorbed pore water is proposed to be necessary for initiating photoinduced hydrolysis reactions and maintaining capillary compressive forces between particles. Given an equivalent fluence (20 J cm^{-2}) above the band gap onset, harder films were obtained using successively shorter wavelengths, in agreement with measured absorptivity data for titania xerogel films. The data indicate that photoreactive sintering processes lead to permanent bond formation in our wetted xerogel films.

Introduction

Titania has become a broadly studied wide band gap semiconductor. This is largely due to extensive applications focusing on its function not only as the leading pigment for the paint industry but also as a photocatalytic oxidant of pollutants in air and water, for self-cleaning glass coatings, as varistor circuits in electrical components, as biocompatible coatings for bone implants, and as a component in photovoltaics.[1−6] We further note that the effects of a given sol preparation technique on coarsening and surface area loss in titania films are significant for the next generation solar cells, the dye-sensitized "Grätzel cell" that uses nanoparticulate TiO_2 for charge transfer.[6] Maintaining a high surface area is particularly important in this case, as the significant portion of the material reacting to the absorption of light is the interfacial monolayer of dye. New developments in flexible dye-sensitized cells deposited on polyethylene teraphthalate (PET) polymers have generated increased interest in processing films at lower temperatures than conventional thermal sintering.[7−9] Also, given the extensive importance of titania in new air and water purification systems, self-cleaning glass, and solar cell devices, research related to the surface modification and photoinduced alteration of these films is invaluable. As such, the mechanisms of bonding and growth under UV irradiance are fascinating avenues of research.

High-energy light sources have been applied recently for the crystallization and densification of sol−gel-derived metal oxides.[10−13] Humidity was found to be an important cooperative component with supraband gap light, but a controlled systematic study of this variable under isothermal conditions was inadvertently missed.[10] Additionally, the solvent used in sol preparation has been known to be critical to the crystallinity and derived phase of titania,[14] yet this parameter has not been addressed in view of prior photonic crystallization studies. Thus, a thorough study, which specifically addresses the parameters of sol preparation, levels of relative humidity, and discrete applied energy levels (i.e., specific wavelengths) for a given metal oxide, has not yet been accomplished.

* Corresponding author. Tel.: 1 608 262 2674. Fax: 1 608 262 0454. Email: nanopor@wisc.edu.

(1) Bahnemann, D. W.; Mönig, J.; Chapman, R. *J. Phys. Chem.* **1987**, *14*, 3782.
(2) Hoffmann, M. R.; Martin, S. T.; Choi, W.; Bahnemann, D. W. *Chem. Rev.* **1995**, *95*, 69.
(3) Wang, R.; Hashimoto, K.; Fujishima, A.; Chikuni, M.; Kojima, E.; Kitamura, A.; Shimohigoshi, M.; Watanabe, T. *Nature* **1997**, *388* (6641), 431.
(4) Kormann, C.; Bahnemann, D. W.; Hoffmann, M. R. *J. Phys. Chem.* **1998**, *92*, 5196.
(5) Nosaka, Y.; Kishimoto, M.; Nishino, J. *J. Phys. Chem. B* **1998**, *102*, 10279.
(6) O'Regan, B; Grätzel, M. *Nature* **1991**, *353*, 737.
(7) Pichot, F.; Pitts, J. R.; Gregg, B. A. *Langmuir* **2000**, *16*, 5626.
(8) Oekermann, T.; Zhang, D.; Yoshida, T.; Minoura, H. *J. Phys. Chem. B* **2004**, *108*, 2227.
(9) Miyasaka, T.; Kijitori, Y. *J. Electrochem. Soc.* **2004**, *151* (11), A1767.
(10) Imai, H.; Hirashima, H.; Awzu, K. *Thin Solid Films* **1999**, *351*, 91.
(11) Asakuma, N.; Fukui, T.; Aizawa, M.; Toki, M.; Imai, H.; Hirashima, H. *J. Sol−Gel Sci. Technol.* **2000**, *19*, 333.
(12) Asakuma, N.; Hirashima, H.; Imai, H.; Fukui, T.; Maruta, A.; Toki, M.; Awazu, K. *J. Appl. Phys.* **2002**, *92* (10), 5707.
(13) Ohya, T.; Nakayama, A.; Ban, T.; Ohya, Y.; Takahashi, Y. *Bull. Chem. Soc. Jpn.* **2003**, *76*, 429.
(14) Hague, D. C.; Mayo, M. J. *J. Am. Ceram. Soc.* **1994**, *77* (7), 1957.

10.1021/cm050082w CCC: $30.25
Published on Web 05/07/2005

The sol−gel route of producing metal oxide thin films has proven to be a relatively inexpensive method of the synthesis and deposition of these materials. Sols can be generated by both acid- or base-catalyzed hydrolysis and the subsequent condensation of titanium alkoxide precursors, yielding charge-stabilized suspensions of 3−10-nm particles.[15,16] Nanoparticles within the xerogel film possess an higher excess surface energy due to increased surface stress from bond distortion, described in detail by Banfield and Zhang,[17] which can be lowered by forming interparticle bonds (sintering) or chemical bonds with other surface species. In the case of TiO_2 (anatase phase), the surface stress-modified excess surface energy per gram of solid (γ_e) can be estimated at 4.23×10^{21} eV/g (678 J/g) (eq 1) where γ is the average surface energy of anatase at 298 K considering surface stress contributions (8.24 eV/nm^2 or 1.32×10^{-4} J/cm^2), r is the particle radius (1.5 nm), and ρ is the density of anatase (3.893×10^{-21} g/nm^3 or 3.893 g/ cm^3).[17,18] However, as the radius r increases to larger values of 10 or 100 nm, γ_e is reduced to 6.35×10^{20} (102 J/g) or 6.35×10^{19} eV/g (10 J/g), respectively. For nanoparticles with extremely high surface area/volume ratios such as ours, the particle radii are small ($1.5 \text{ nm} < r_{\text{particle}} < 5$ nm) and the excess surface energy is quite high. Bond formation with other species is expected to be extremely favorable under the appropriate conditions.

$$\gamma_e = \frac{3\gamma}{r\rho} = 4.23 \times 10^{21} \text{ eV/g} = 678 \text{ J/g} \qquad (1)$$

To prepare a crystalline anatase sol, the presence of an acid catalyst and an excess of water are necessary to bring about a complete hydrolysis of the precursor material.[15] It has also been reported that an excess of alcohol within the initial hydrolysis reaction will lead to an amorphous titania sol/gel.[14] This is largely due to the reversible nature of the acid-catalyzed hydrolysis/esterification reaction and the high surface areas available for reactivity (eq 2).[19−21] The term *esterification* is used due to its parallel with the reversible carboxylic/alcohol substitution reaction in pure organic nomenclature. One exploits Le Chatelier's principle to enable a forward reaction favoring a hydroxide-terminated surface, which ultimately leads to a thermodynamically stable anatase nanocrystal. Once hydrolysis and condensation are complete, a particulate oxide remains with a hydroxide-terminated surface. However, the subsequent introduction of excess alcohol within the particulate suspension can elicit a re-esterification or transesterification of the hydroxide surface by the same principle. This is a well-documented phenomenon for silica gels[19,20] but is only recently receiving attention via the enigma of "reversible wettability" for a titania surface.[21] Burgos and Langlet have found transesterification of the isopropyl groups with ethoxy groups on the titania surface.[22] Wang et al. have also confirmed methoxy groups on the titania surface following methanol vapor adsorption using surface-specific SFG spectroscopy, and have calculated methanol chemisorption to be barrierless thermodynamically.[21] After altering the surface chemistry, these nanoparticles have been found to relax into either an X-ray diffraction amorphous coating, or an entirely amorphous nanoparticle.[14]

$$\equiv \text{Ti}-\text{OR} + \text{H}_2\text{O} \underset{\text{esterification}}{\overset{\text{hydrolysis}}{\rightleftharpoons}} \equiv \text{Ti}-\text{OH} + \text{ROH} \qquad (2)$$

As the importance of titanium dioxide grows in terms of its use as a novel stable material in photocatalytic and photovoltaic applications, our goal to produce quality uniform films on an increasing variety of substrates has been challenged. Recent "low-temperature sintering" methods have proposed the addition of a surfactant or titanium precursor into the pore space. However, this process may lower the surface areas of the films and hence affect their reactivity.[7−9] In fact, this step may be *bypassed*. It is by taking advantage of the reversible properties of the sol−gel process and the photoreactive properties of TiO_2 that we have been able to provide a simple third route of film hardening that bypasses this precursor addition. In this paper, we demonstrate a UV-induced hardening effect in surface-modified titania films.

Experimental Procedures

Film Synthesis. The titanium dioxide particles in this study were synthesized by rapid hydrolysis and condensation of a pure Ti(IV) tetraisopropoxide ($Ti(O^iPr)_4$) precursor in ultrapure water catalyzed by nitric acid (200 mL of H_2O/33 mL of $Ti(O^iPr)_4$/1.43 mL of concentrated HNO_3), then peptized in the acidic aqueous solution for 5 days, and subsequently dialyzed against ultrapure water to a pH of ∼2.3. The resulting suspension of 3−10-nm TiO_2 particles (∼32 g/L) were charge stabilized and developed from a sol of amorphous nanoparticles to that of crystalline anatase nanoparticles within the first few days of synthesis (aging at room temperature). These data were confirmed in an earlier study.[15,16] Once generated, the sols were stored in a dark, refrigerated (4 °C) environment until needed for coating.

Coating was performed using a novel low-pressure ultrasonic spray system from Sono-Tek, Inc. Titania sols were diluted with ethanol (ethanol/water molar ratio ≈ 1, 75% ethanol by volume, 8 g/L solid content). The diluted sol was then passed through a 0.2-μm polytetrafluoroethylene filter to remove any large contaminants that might seed the crystallization process. This suspension was subsequently loaded into 60-mL syringes for syringe-pump delivery of the sol to the ultrasonic horn. The ethanol lowered the surface tension of the suspension for spray deposition, promoting the quick drying of the film, and changed the solvent environment of the titania particles. Subsequent sol dilutions (8 g/L solid content) employing a 0.5 and 0.67 ethanol/water

(15) Xu, Q. Ph.D. Thesis. University of Wisconsin-Madison: Madison, WI, 1991.
(16) Xu, Q.; Anderson, M. A. *J. Mater. Res.* **1991**, *6* (5), 1073.
(17) Zhang, H.; Banfield, J. F. *J. Mater. Chem.* **1998**, *8* (9), 2073.
(18) Chiang, Y.-M.; Birnie, D. P., III; Kingery, W. D. *Physical Ceramics: Principles for Ceramic Science and Engineering;* MIT Series in Materials Science and Engineering, John Wiley & Sons: New York, 1997.
(19) Brinker, C. J.; Scherer, G. W. *Sol−Gel Science: The Physics and Chemistry of Sol−Gel Processing*; Academic Press: Boston, MA, 1990.
(20) Brinker, C. J. *J. Non-Cryst. Solids* **1988**, *100*, 31.
(21) Wang, C.; Groenzin, H.; Schulz, M. J. *J. Phys. Chem. B* **2004**, *108*, 265.
(22) Burgos, M.; Langlet, M. *Thin Solid Films* **1999**, *349*, 19.

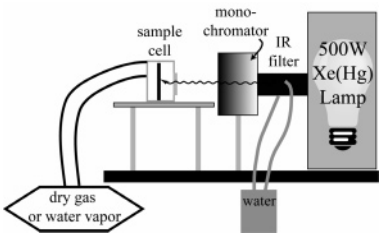

Figure 1. Schematic of UV reactor.

molar ratio were later prepared for comparison. The system used for spraying delivered uniform coatings on glass slides that gelled quickly and had thicknesses between 150 and 300 nm as determined by ellipsometry. Films were used within two weeks of coating and stored under dry conditions.

Absorptivity. Separate titania thin films were created by pipetting a small volume of an ethanol-diluted titania sol onto a clean quartz slide (10 μL of 5.125 g/L, coated over an area of 12.26 cm^2). On the basis of the deposited volume and solid concentration in the sol, a film of known mass was distributed over the measured area (1.67×10^{-5} g/cm^2). By assumption of a density of anatase (3.893 g/cm^3), we then calculated the mean solid thickness of the deposited film as 43 nm. Effective film-thickness and porosity were concurrently established from ellipsometry measurements of the same film. The film was found to have a thickness of approximately 98 nm with an index of refraction of 1.69. Porosity and effective film thickness was estimated using the index of refraction of solid anatase (3.55) obtained from the literature. A porosity of 56% and a solid thickness of 43.8 nm were calculated from the measured index. This was in reasonable agreement with the calculated thickness based on pipetted mass.

UV−vis absorbance of the titania films was then measured using a Hewlett-Packard HP8452a photodiode array spectrophotometer. The coated slides were mounted perpendicular to the light beam, and film absorbance was recorded for several spots over the area of the coated slide. Corrections were made for the absorbance of the quartz (though this was minimal) and reflections from the surfaces. The absorbance measurements were then normalized to the thickness of the titania solid to yield absorptivity data (absorbance/nm).

Photoreactor Design. A reactor for controlled temperature and relative humidity (RH) was constructed in line with a high-irradiance monochromatic light source (Figure 1). A 500-W Oriel Xe(Hg) arc lamp capable of 200−600-nm excitation wavelengths (with ozone venting) was used as the light source. Source light was first passed through a water-cooled IR filter and then on through a Czerny-Turner-style monochromator (with 3-mm slit widths on both sides).

The main reactor was a UV opaque Plexiglas box (28.32 L/1 ft^3) with side gas ports for humidity control. A 50 mm diameter fused silica window (UV transparent) was installed to allow a full spectrum of high-energy light to pass into the reactor. Coated samples were mounted behind the UV window perpendicular to the light source for UV exposure and off to the side for dark exposures. Irradiance of the selected wavelength was recorded between tests using a wavelength-specific calibrated digital photometer (International Light, Inc.) for absorptivity calculations and also to confirm the absence of drift in light intensity over the period of fluence.

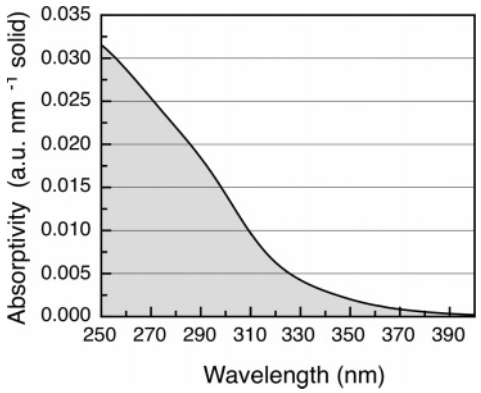

Figure 2. Absorptivity of room-temperature-dried nanoparticulate TiO_2 film on quartz, normalized to the effective thickness of the solid (nonporous) portion of the film.

The reactor was humidified by passing ~2 L/min of medical-grade air through two glass diffusers containing ultrapure water (>18 MΩ cm). Internal silicone-coated heat tape and a 2.5-W fan created a well-mixed environment within the reactor. Reactor temperature and relative humidity data were collected by a Vaisala HMP235 probe. System control was enabled using a National Instruments SC-2345 I/O system and PCI-603 6E DAQ Card, and temperature and RH data were logged each minute via LabVIEW software. The experimental conditions remained stable over the duration of the experiments.

UV Exposure. For experiments designed to test the change in film characteristics under different RH values, 300-nm light (4.13 eV) was selected and a 3-h UV exposure was employed. Experiments were performed at 40 °C at relative humidities of <3, 25, and 40%. Films were placed in the reactor and allowed to equilibrate at reactor temperature and relative humidity for approximately 1.5 h before being exposed to UV light. The exposed spot size was approximately 1 cm by 0.5 cm. Average irradiance at the sample surface was 3.19 (±0.31) mW cm^{-2}, yielding an approximate fluence of 34.5 J cm^{-2} (or 345×10^3 J m^{-2}) for each experiment. Control experiments were performed synchronously for dark exposure, to test the response of the films to nonirradiated conditions at 40 °C and the defined relative humidity.

Experiments testing the change in films under different UV energies/wavelengths were performed at 40 °C and 40% RH. Films were exposed to an equivalent fluence of 20 J cm^{-2} for each wavelength of 254, 300, 350, and 378 nm, as confirmed by calibrated irradiance measurements. Wavelengths of 254 and 378 nm were specifically selected as bounds for the peak irradiance of a UVB germicidal Hg fluorescent bulb and the band gap onset for anatase.

Characterization of UV Films. Following test exposures, the films were subjected to pencil scratch tests by using 9H-9B Derwent Graphic pencils (Acco UK, Ltd.). The pencil test follows an ASTM standard procedure #D3363 for testing relative film hardness. Beginning with the hardest pencil (9H), the pencil is held at 45° and pushed away from the tester in a 1-cm stroke on a flat surface. If the pencil gouges and scribes the film, the next softer pencil is used, on down

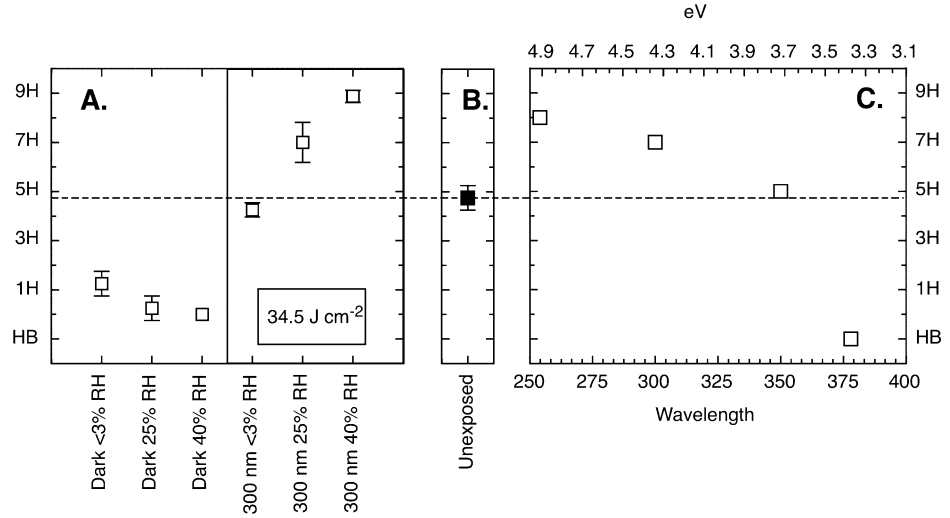

Figure 3. Left: Pencil hardness results for 300-nm UV exposure. All films were exposed to 3 h of 40 °C at a given RH in the presence of UV (34.5 J cm^{-2}) or darkness. Center: Unexposed films. Right: Pencil hardness results for equivalent fluence per area (20 J cm^{-2}) given 40% RH.

to the pencil that does not scribe the film. This is termed the pencil hardness and is a measure of the structural integrity of the film as a whole. Because of the porous nature of the film, some graphite is embedded in the process for the softer pencils, but atomic force microscopy (AFM) was used to confirm this did not scratch the film. The tests were repeated in four to five replicate experiments to establish relative film hardness at each humidity setting.

Contact-angle measurements were performed immediately after each exposure, using ~10 μL of ultrapure water dropped by a micrometer-driven syringe onto the film on a horizontal base. These tests were also replicated multiple times to establish a significant data set. Contact angles were subsequently monitored periodically for the next 14 days to note any changes over time. Contact angles are strongly dependent upon adsorbed surface species. Therefore, we also analyzed the organic surface species by transmission Fourier transform infrared (FTIR) spectroscopy. Sol−gel-derived TiO_2 thin films were spray deposited on Si wafer substrates as described for the glass substrate. Mesoporous films from sol−gel-derived titania greatly enhance the surface signal for spectral analyses, again due to their extremely high surface area per mass, such that the spectra accurately approximate a surface-specific technique. Analyses were performed on dried films before and after 20 J cm^{-2} UV exposure (254 nm, 40 °C, 40% RH).

The structure of the sample films was characterized by tapping-mode AFM and reflected light microscopy. AFM was performed on both the dark and UV-exposed areas for the 40% RH and the dry experiments using a Digital Instruments 31000 AFM. SiN tips were used to scan a 500 × 500 nm^2 area at 1 Hz and 512 scan lines per image.

Results

The absorptivity (normalized to the thickness of the actual solid portion of the titanium dioxide) for an unsintered nanoparticulate TiO_2 film on quartz is shown in Figure 2. The spray-coated TiO_2 films used in the UV exposure study have thicknesses of approximately 100 nm and porosities of approximately 50%, as determined by ellipsometry. From these data, we can calculate the absorptivity of the sprayed films. For a 100 nm thick film (50 nm of solid anatase) at wavelengths of 254, 300, 350, and 378 nm, the resulting absorbances were 1.53, 0.71, 0.10, and 0.03, respectively.

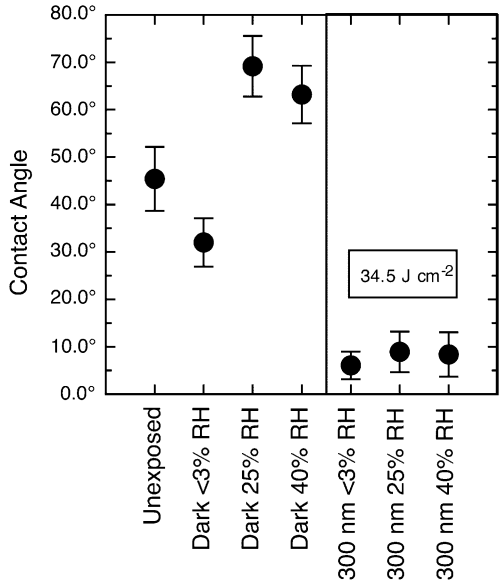

Figure 4. Water/film contact-angle results for 300-nm UV exposure. All nonambient films were exposed to 3 h of 40 °C at a given RH in the presence of UV or darkness.

Films generated from a sol with an ethanol/water molar ratio of ~1 were found to be significantly harder when exposed to both a humidified environment (25 and 40% RH) and UV irradiance (3 h, 300 nm, 34.5 J cm^{-2} exposure) relative to unexposed controls (Figure 3A). Films appeared to increase in hardness with increasing humidity as well, and films at 40% RH tended to register at the upper limit of the pencil testing apparatus. Film-hardness did not significantly increase for UV exposures with <3% RH (dry). Films exposed in the dark to various humidity environments (<3, 25, and 40% RH) at a fixed 40 °C temperature did not show any increase in hardness. In fact, these films actually all became softer with exposure to 40 °C heat under all humidity conditions. Films generated from sols with a molar ratio of 0.5 and 0.67 both altered from 5H to 6H under optimal

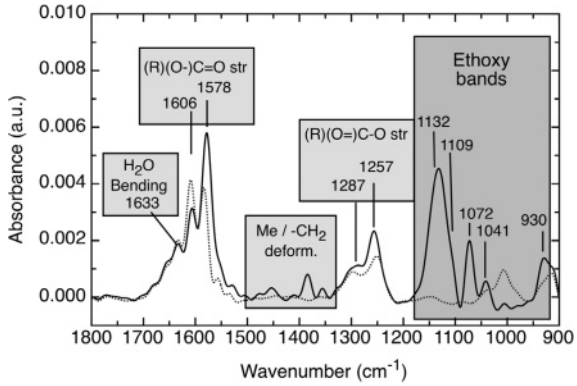

Figure 5. FTIR spectra of TiO_2 film from ethanol dilution. Dark solid line is the film prior to UV treatment (20 J cm^{-2}, 254 nm, 40 °C, 40% RH). Dotted line is the film post-UV treatment.

conditions of 254 nm (20 J cm^{-2}), 40 °C, 40% RH. There was no significant difference in the film hardness between UV and dark regions for these tests. Compared with the increase to 8H hardness under the same conditions for sols with a molar ratio of ~1, this was minimal hardening for the lower alcohol ratio.

Contact angles of <10° were found in all films exposed to UV, regardless of humidity level (Figure 4). The same areas were periodically measured over a two-week period of resting under ambient lighting conditions in a laminar flow hood, and contact angles were found to slowly increase in all UV cases. Films exposed to dark conditions at 40 °C showed an increase in contact angles if exposed to more humidity relative to unexposed controls (25 and 40% RH). The dry (<3% RH) dark controls did not show a significant change in contact angle relative to unexposed controls. The incident irradiances of these wavelengths for the films within our UV reactor were measured as 3.03, 3.19, 1.78, and 0.73 mW cm^{-2} for the same respective wavelengths. Given these data, the experiments performed with 254-nm radiation were predicted to have absorbed 97.0% of the incident photons, whereas for 300 nm, 80.1% of the incident light was absorbed, for 350 nm, 20.7% of the incident light was absorbed, and at 378 nm, only 6.7% of the incident light was absorbed. In close agreement with these data, Figure 3C demonstrated a decrease in film hardness with increasing incident wavelength for films exposed to an equivalent fluence (20 J cm^{-2}). In fact, the experiment for 378 nm showed the same results as were found in the dark exposures of the relative humidity tests; the film actually lost structural integrity relative to the unexposed controls.

FTIR spectroscopy of the films on Si substrates revealed C−O and C−C bands (930, 1041, 1072, 1109, and 1132 cm^{-1}) consistent with those found by both Burgos and Langlet[22] and Wu et al.[23] regarding ethanol adsorption and esterification of anatase surfaces (Figure 5). Specifically, the bands at 930 and 1072 cm^{-1} are unique to ethoxide species. Carboxylate bands (1578 and 1606 cm^{-1}) potentially matching formate and acetate moieties were also discovered on the surface of the dried films prior to UV exposure. As these are typical residual oxidation products of primary alcohols and alkoxides, these species were not surprising. Tests

(23) Wu, W.; Chuang, C.; Lin, J. *J. Phys. Chem. B* **2000**, *104*, 8719.

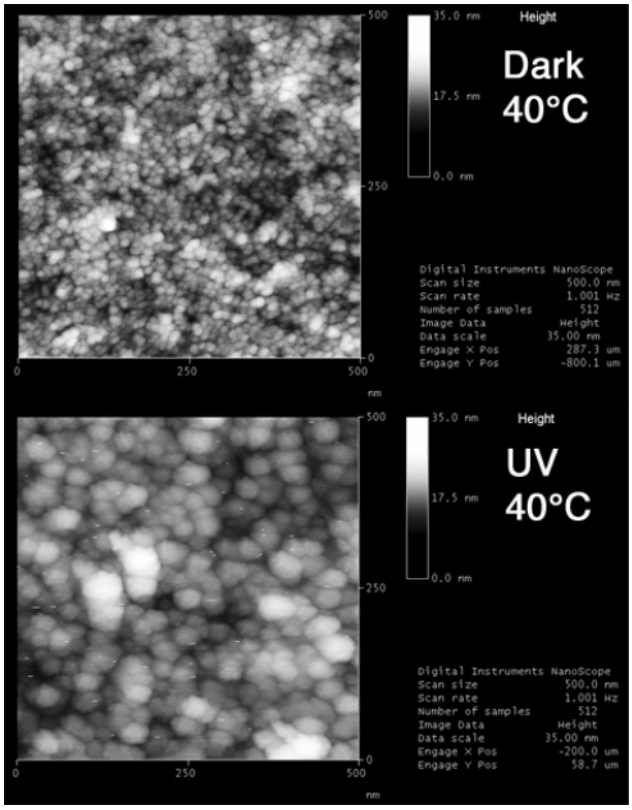

Figure 6. AFM images of films. Top image ("Dark 40 °C") is that of 3-h dark exposure of TiO_2 film to 40 °C at 40% RH. Particle size is ~14−15 nm in diameter. Lower image ("UV 40 °C") is that of 3-h UV exposure of TiO_2 film to 40 °C, 40% RH, and 300 nm light (34.5 J cm^{-2}). Particle size is between 38 and 51 nm, two to three times primary particle size.

confirmed that the ethoxy species were oxidized and removed and carboxylate species decreased given a 20 J cm^{-2} fluence at 254 nm. Formate species that showed an initial increase were later confirmed to also decrease with more UV exposure (not shown). Control tests of completely inorganic TiO_2 films show negligible surface organic species and no hardening or growth effects.

AFM indicated a definite increase in mean particle size when comparing the UV-exposed area of a slide with the non-UV-exposed area of the slide in the 40% RH samples (Figure 6). The non-UV-exposed area appeared to be composed of 14−15-nm diameter particles. In contrast, the UV-exposed area of the slide showed larger aggregated particles between 38 and 51 nm in diameter. We found no observable difference between treated and untreated samples nor between the samples exposed to different UV energies using reflected light microscopy.

Discussion

Sol−gel-derived thin films have small particle and pore radii and high surface area/volume ratios, making porous thin-film systems prone to lowering of particle surface free energies via bond formation and particle growth. It is important to recognize that the sol preparation method drives the surface chemistry of the titania nanoparticles. When synthesized in an alcoholic medium, the resulting particles are amorphous.[14] However, when the sol is synthesized in an excess of water with an acid catalyst, the resulting nanoparticles stabilize into the anatase phase after several

days.[15] The surface functionalization and crystallinity can be easily reversed by a wash in the appropriate medium and have been documented by Hague and Mayo in a comparison of several earlier titania synthesis studies.[14] We propose that the chemical bonding of alcohols through acid-catalyzed re-esterification of the titania surface can be brought about in an acidic ethanolic environment and is easily reversible for protic, polar solvents such as methanol and ethanol. A small molar ratio of ethanol/water such as 0.5 and 0.67 leaves an excess of water in the pores to favor the reaction toward surface hydrolysis. Establishing a molar ratio ≈ 1 results in increased efficiency of surface esterification. Once functionalized with alkoxy groups, the surface has been found to remain stable as long as the sample is maintained relatively free of water and under dark conditions.

Both light and humidity are necessary for the photoactivated hardening process. Supraband gap energy excitation of titania thin films in the presence of condensed water within the pore space will then lead to low-temperature nanoparticle surface hydrolysis, aggregation, and growth. AFM characterization following UV exposure under humid conditions has demonstrated particles having two to three times the primary titania particle size for experiments with UV exposure. This increase in particle size has confirmed that crystal growth occurs via this photonic process. This is likely a complex cooperation of chemical and nonconservative frictional forces (e.g., capillarity).

The initial stages of aging and drying of a gel (and sintering) involve consolidating a body (in this case a thin film) comprised of particles through a process of syneresis (shrinkage) followed by densification with pore elimination.[24] The wetting liquid concentrated at the particle−particle grain interface exerts a strong capillary compressive pressure to pull the particles together, rearranging the particles in an initial burst of densification. Hydrolyzed xerogel thin films have a hydrated pore structure, bearing water layers at relatively low relative humidities.[25] Capillary compressive forces within xerogel pores are expected to be high with the presence of water due to small pore size (e.g., ~97 MPa for water in a 3 nm diameter spherical pore). For nanoparticles at low temperatures, the densification may proceed until excess surface energies match the work exerted by capillary compressive force per volume.

UV light has been found to lower the water/titania contact angle in the porous films. This allows continual wetting throughout the tight and tortuous pore structure and an extended contribution to capillary compressive forces, bringing the particles together initially. Hence, in the absence of pore water condensation there is less capillary compressive force within the pores and particles do not have the mesoscopic motility to migrate across pore vacancies.

The pore water serves a dual purpose, however; it also enhances photoreactions with surface organics. A liquid additive aids sintering if it possesses an ability to maintain a low contact angle, indicating that it will wet and penetrate between the particles leading to rearrangement and densification and partially react with the titania/ethoxy surface.[18,26] UV light can modify the titania surface by oxidizing the surface chemistry from initial amorphous ethoxy functional groups, leading to crystalline anatase in the resulting gel.[27] This is in agreement with SFG spectroscopy data[20] and general titania photocatalysis knowledge and would help to explain the "reversible wettability" observed for titania films.

Our FTIR spectra show the initial presence of ethoxy species on the titania surface and oxidation products following both drying and 20 J cm^{-2} UV irradiation. The additional carboxylate species are logical oxidation products of both primary alcohols and surface ethoxides. Hence, the presence of carboxylates immediately after drying indicates that the titania particles have a highly reactive surface even under the negligible lighting conditions of thin film preparation, which is then greatly accelerated and enhanced with the addition of supraband gap light and humidity. The residue following ethoxide and carboxylate oxidation indicates either the possible entrapment of organics within the pore structure, or incomplete oxidation/mineralization of the surface organics. Future research will focus on identifying the species on the TiO_2 surface following esterification.

Absorptivity data also indicate that more light is absorbed in the films for higher-energy incident photons. The light-absorbing efficiency of the films increased from 6.7 to 97.0% as wavelengths decreased from 378 to 254 nm, and the resulting films became harder under an equivalent fluence of incident photons. We propose a connection between the quantum efficiency of photocatalytic hydrolysis of surface alkoxide groups and the hardening of titania films. This is significant from an application standpoint, considering that 254-nm wavelength light is emitted by standard germicidal fluorescent UV bulbs (uncoated Hg vapor lamps), which are additionally more energy efficient at higher pressures (e.g., for industrial processing lamps). Low-temperature UV sintering of titania films may be best performed with these readily available bulbs. This opens up possibilities for energy efficient post-treatment of temperature-sensitive surfaces for photocatalysis and photovoltaics.

Acknowledgment. The authors sincerely thank Cardinal CG Co. (Eden Prairie, MN) for their financial support and positive discussions regarding this research. Thanks to Dr. Isabel Tejedor-Tejedor for positive discussions regarding infrared spectral analyses.

CM050082W

(24) Scherer, G. W. *J. Non-Cryst. Sol.* **1988**, *100*, 77.
(25) Vichi, F. M.; Tejedor-Tejedor, M. I.; Anderson, M. A. *Chem. Mater.* **2000**, *12* (6), 1762.
(26) German, R. M. *Sintering Theory and Practice*; John Wiley & Sons: New York, 1996.
(27) Liu, H.; Yang, W.; Ma, Y.; Cao, Y.; Yao, J.; Zhang, J.; Hu, T. *Langmuir* **2003**, *19*, 3001.